V International Conference on Computational Methods for Coupled Problems in Science and Engineering
COUPLED PROBLEMS 2013
S. Idelsohn, M. Papadrakakis and B. Schrefler (Eds)

PROBABILITY AND VARIANCE-BASED STOCHASTIC DESIGN OPTIMIZATION OF A RADIAL COMPRESSOR CONCERNING FLUID-STRUCTURE INTERACTION

DIRK ROOS*, KEVIN CREMANNS & TIM JASPER

Institute of Modelling and High-Performance Computing
Niederrhein University of Applied Sciences
Reinarzstr. 49, D-47805 Krefeld, Germany
e-mail: dirk.roos[@]hs-niederrhein.de

Key words: robust design optimization, robustness evaluation, reliability analysis, fluid-structure interaction, surrogate models, adaptive design of experiment, importance sampling, directional sampling

Abstract. Since the engineering of turbo machines began the improvement of specific physical behaviour, especially the efficiency, has been one of the key issues. However, improvement of the efficiency of a turbo engine, is hard to archive using a conventional deterministic optimization, since the geometry is not perfect and many other parameters vary in the real approach.

In contrast, stochastic design optimization is a methodology that enables the solving of optimization problems which model the effects of uncertainty in manufacturing, design configuration and environment, in which robustness and reliability are explicit optimization goals. Therein, a coupling of stochastic and optimization problems implies high computational efforts, whereby the calculation of the stochastic constraints represents the main effort. In view of this fact, an industrially relevant algorithm should satisfy the conditions of precision, robustness and efficiency.

In this paper an efficient approach is presented to assist reducing the number of design evaluations necessary, in particular the number of nonlinear fluid-structure interaction analyses. In combination with a robust estimation of the safety level within the iteration and a final precise reliability analysis, the method presented is particularly suitable for solving reliability-based structural design optimization problems with ever-changing failure probabilities of the nominal designs.

The applicability for real case applications is demonstrated through the example of a radial compressor, with a very high degree of complexity and a large number of design parameters and random variables.

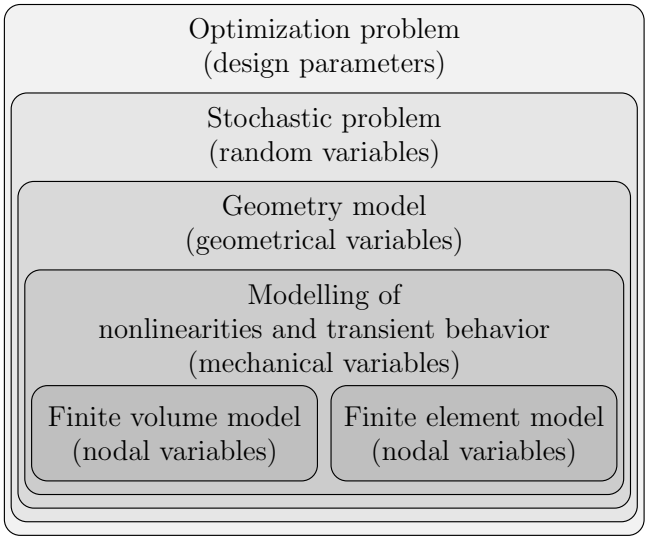

Figure 1: Coupled numerical models and different variable spaces of a stochastic design optimization of a fluid-structure interaction analysis based on a parametric geometry model (according Chateauneuf, 2008).

1 INTRODUCTION

1.1 Stochastic design optimization

In engineering problems, randomness and uncertainties are inherent and may be involved in several stages, for example in the system design with material parameters and in the manufacturing process and environment. Stochastic optimization, also referred to as reliability-based and variance-based optimization is known as the most adequate and advantageous methodology for system or process design and aims at searching for the best compromise design between design improvement and robustness or reliability assurance, considering uncertainties of geometry, material, manufacturing and process. Herein, the optimization process is carried out in the space of the design parameters and the robustness evaluation and reliability analysis are performed in the space of the random variables. Consequently, during the optimization process the design variables are repeatedly changed, whereby each design variable vector corresponds to a new random variable space. Therefore usually, a high number of numerical calculations are required to evaluate the stochastic constraints at every nominal design point. This repeated search becomes the main problem, especially when numerical nonlinear multi-domain simulations and CAD models are involved.

Unfortunately, in real case applications of the virtual prototyping process, it is not always possible to reduce the complexity of the physical models to obtain numerical models which can be solved quickly. Usually, every single numerical simulation takes hours or even days. Although progress has been made in identifying numerical methods to solve stochastic design optimization problems and high performance computing, in cases such as those that have several nested numerical models, as shown in Fig. 1, the actual costs of using these methods to explore various model configurations for practical applications is too high. Therefore, methods for efficiently solving stochastic optimization problems based on the introduction of simplifications and special formulations for reducing the numerical efforts are required.

1.2 Application to aerodynamic optimization

In comparative studies on the application of the deterministic optimization for aerodynamic optimization (see e.g. Müller-Töws, 2000, Sasaki et al., 2001, Shahpar, 2000) usually stochastic programming algorithms or response surface methods (see e.g. Pierret and van den Braembussche, 1999) are used in turbomachinery design, for example in the development of engine components, such as at Vaidyanathan et al. (2000). In Shyy et al. (2001) a comprehensive overview is represented.

An example of an applied aerodynamic deterministic optimization using a genetic algorithm is published in Trigg et al. (1997) and the optimized design of transonic profiles also using genetic algorithms is given in Oyama (2000). Another very comprehensive study of the use of the combination of genetic algorithms and neural networks for two-dimensional aerodynamic optimization of profiles is presented in Dennis et al. (1999) combine a genetic algorithm with an gradient-based optimization method.

Furthermore, an increasing application of stochastic analysis on turbo machinery (e.g. at Garzon, 2003, Garzon and Darmofal, 2003, Lange et al., 2010, Parchem and Meissner, 2009) underlines the importance of integrating the uncertainty analysis into the aerodynamic design process.

2 RELIABILITY AND VARIANCE-BASED DESIGN OPTIMIZATION

2.1 Deterministic optimization

Optimization is defined as a procedure to achieve the best outcome of a given objective function (sometimes also called cost function) while satisfying certain re-

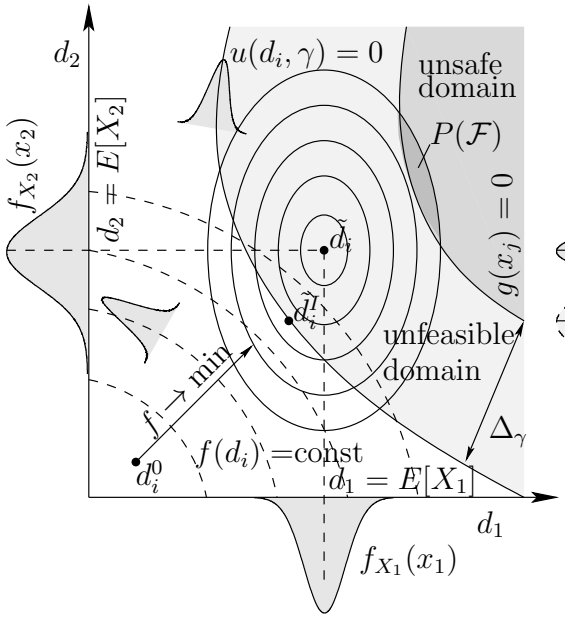

Figure 2: Different solution points $\tilde{d}_i^I$ or $\tilde{d}_i$ as result of a deterministic vs. stochastic design optimization in the space of given randomly distributed design parameters.

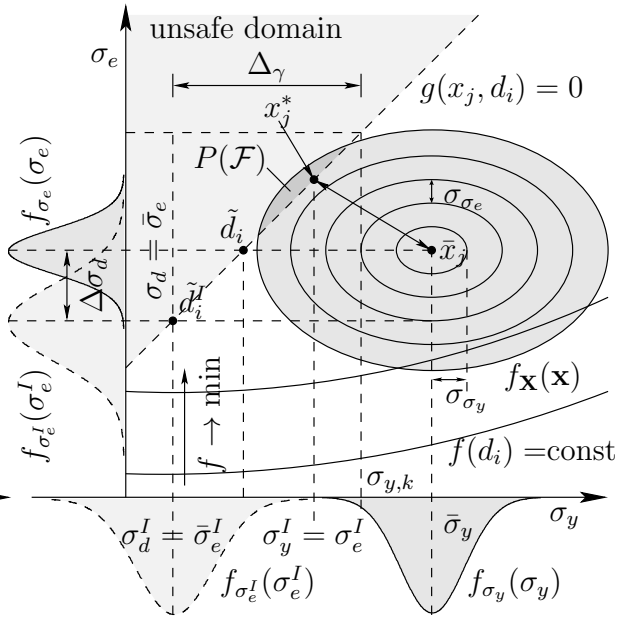

Figure 3: Comparison of the deterministic optimal point $\tilde{d}_i^I$ and the solution of a stochastic optimization $\tilde{d}_i$ with corresponding most probable failure point x_j^* in the space of the randomly distributed von Mises stress and the yield stress.

strictions. The deterministic optimization problem

$$\begin{aligned} f(d_1,d_2,\dots d_{n_d}) &\to \min \\ e_l(d_1,d_2,\dots d_{n_d}) &= 0;\ l=1,n_e \\ u_m(d_1,d_2,\dots d_{n_d},\boldsymbol{\gamma}) &\geq 0;\ m=1,n_u \\ d_{l_i} \leq d_i &\leq d_{u_i} \\ d_i \in [d_{l_i},d_{u_i}] &\subset \mathbb{R}^{n_d} \end{aligned} \tag{1}$$

is defined by the objective function $f:\mathbb{R}^{n_d}\to\mathbb{R}$ subject to the restrictions, defined as equality and inequality constraints e_l and u_m. The variables $d_1,d_2,\dots d_{n_d}$ are the optimization or design variables and the vector of the partial safety factors $\boldsymbol{\gamma}$ ensures the system or design safety within the constraint equations u_m, for example defining a safety distance $u(\mathbf{d},\gamma)=y_g/\gamma-y_d\geq 0$ between a defined limit state value y_g and the nominal design value y_d of a physical response parameter $y=f(\mathbf{d})$. In structural safety assessment, a typical constraint for the stress is given as

$$u(\mathbf{d},\gamma)=\sigma_{y,k}/\gamma-\sigma_d\geq 0 \tag{2}$$

ensuring the global safety distance

$$\Delta_\gamma = \sigma_{y,k} - \sigma_d = \sigma_{y,k} - \frac{\sigma_{y,k}}{\gamma} = \sigma_{y,k}\left(1 - \frac{1}{\gamma}\right)$$

between the defined quantile value $\sigma_{y,k}$ of the yield stress and the nominal design stress σ_d with the global safety factor γ, as shown in Fig. 3. Whereby, in the real approach with given uncertainties, σ_d corresponds to the mean von Mises equivalent stress $\bar{\sigma_e}$ at the current design point.

2.2 Stochastic chance-constrained optimization

Stochastic optimization algorithms use the quantification of uncertainties to produce solutions that optimize the expected performance of a process or design, ensuring the target variances of the model responses and failure probability. So, the deterministic optimization problem (1) can be enhanced by additional stochastic restrictions. For example, the expression for system reliability

$$1 - \frac{P(\mathcal{F})}{P^t(\mathcal{F})} \geq 0 \tag{3}$$

ensures that the probability of failure

$$P(\mathcal{F}) = P[\{\mathbf{X} : g_k(\mathbf{x}) \leq 0\}] = \int\limits_{g_k(\mathbf{x})\leq 0} \cdots \int f_{\mathbf{X}}(\mathbf{x}) d\mathbf{x} \tag{4}$$

cannot exceed a given target probability $P^t(\mathcal{F})$, considering the vector of all random influences

$$\mathbf{X} = [X_1, X_2, ..., X_{n_r}]^T \tag{5}$$

with the joint probability density function of the random variables $f_{\mathbf{X}}(\mathbf{x})$ and $k = 1, 2, ..., n_g$ limit state functions $g_k(\mathbf{x}) \leq 0$.

These enhancements of the problem (1) are usually referred to reliability-based design optimization, in which we ensure that the design variables d_i satisfy the given constraints (3) to some specified probabilities. As a consequence, now the design parameters

$$\mathbf{d} = E[\mathbf{X}] \tag{6}$$

are the means of the n_r random influences $\mathbf{X}$ with every changing density function during the optimization process. As a result of the random influences, now the objective and the constraints are non-deterministic functions.

2.3 Reliability analysis using adaptive response surface method

For an efficient probability assessment of $P(\mathcal{F})$, according to Eq. (4), a multi-domain adaptive design of experiment in combination with directional sampling (see e.g. Ditlevsen et al., 1990) is introduced in Roos (2011) to improve the accuracy and predictability of surrogate models, commonly used in applications with several limit state conditions. Furthermore, the identification of the failure domains using the directional sampling procedure, the pre-estimation and the priori knowledge of the probability level is no longer required. Therefore this adaptive response surface method is particularly suitable to solve reliability-based design optimization problems considering uncertainties with ever-changing failure probabilities of the nominal designs.

However, a reliability analysis method based on surrogate models, is generally suitable for a few random variables only. In case of the proposed probability assessment method, an efficient application is given up to $n_r = 10, ..., 25$, depending on the number of relevant unsafe domains. Therefore, a variance-based sensitivity analysis should be used to find a reduced space of the important random influences.

2.4 Global variance-based sensitivity analysis

In general, complex nested engineering models, as shown in Fig. 1 contain not only first order (decoupled) influences of the design parameters or random variables but also higher order (coupled) effects on the response parameter of a numerical model. A global variance-based sensitivity analysis, as introduced by Saltelli et al. (2008), can be used for ranking variables $X_1, X_2, \ldots, X_{n_r}$ with respect to their importance for a specified model response parameter

$$Y = f(X_1, X_2, \ldots, X_{n_r})$$

depending on a specific surrogate model $\tilde{Y}$. In order to quantify and optimize the prognosis quality of these meta models, in Most and Will (2008) and Most (2011) the so-called coefficient of prognosis

$$\mathrm{COP} = \left(\frac{\mathbf{E}[Y_{\mathrm{Test}} \cdot \tilde{Y}_{\mathrm{Test}}]}{\sigma_{Y_{\mathrm{Test}}} \sigma_{\tilde{Y}_{\mathrm{Test}}}} \right)^2 ; \quad 0 \leq \mathrm{COP} \leq 1 \tag{7}$$

of the meta model is introduced. In contrast to the commonly used generalized coefficient of determination R^2 based on a polynomial regression model, in Eq. (7) variations of different surrogate models $\tilde{Y}$ are analyzed to maximize the coefficient of prognosis themselves. This procedure results in the so-called meta model of optimal

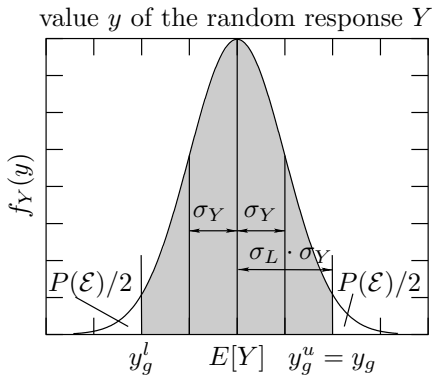

Figure 4: Relationship between density function $f_Y(y)$ of a model response, sigma level and exceedance probability, depending on chosen limit state conditions $y_g^{u,l}$.

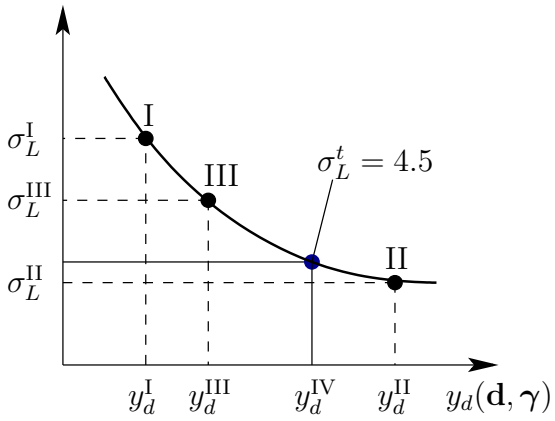

Figure 5: Convergence of a sequential stochastic chance-constrained optimization with successive interpolation of the nominal response limit y_d to ensure a target sigma level σ_L^t.

prognosis, used as surrogate model $\tilde{Y}$ with the corresponding input variable subspace which gives the best approximation quality for different numbers of samples, based on a multi-subset cross validation obtained by latin hypercube sampling (see e.g. Huntington and Lyrintzis, 1998).

The single variable coefficients of prognosis are calculated as follows

$$\mathrm{COP}_i = \mathrm{COP} \cdot \tilde{S}_{T_i} \tag{8}$$

with the total sensitivity indices

$$\tilde{S}_{T_i} = \frac{E(V(\tilde{Y}|\mathbf{X}_{\sim i}))}{V(\tilde{Y})} \tag{9}$$

which have been introduced by Homma and Saltelli (1996), where $E(V(\tilde{Y}|\mathbf{X}_{\sim i}))$ is the remaining variance of $\tilde{Y}$ that would be left, on average, if the parameter of X_i is removed from the model. In Eq. (9) $\mathbf{X}_{\sim i}$ indicates the remaining set of input variables.

2.5 Probability estimation based on moments

For an accurate calculation of the reliability it would be interesting to expand the probability density function of the model responses about a critical threshold. Unfortunately, the density functions are unknown, especially close to the unsafe domain with high failure probability. Existing methods such as polynomial expansions,

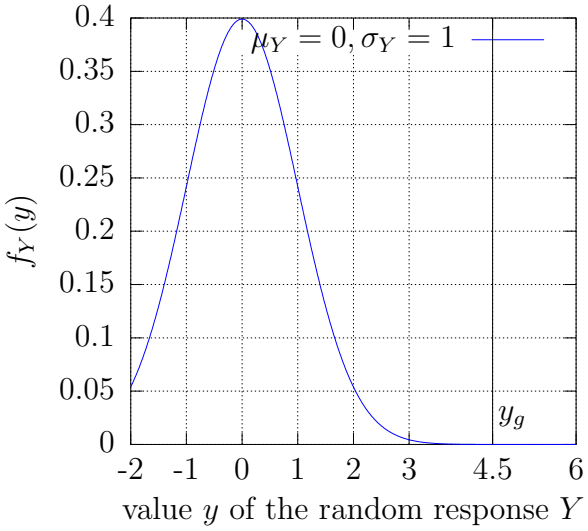

Figure 6: Gaussian density function $f_Y(y)$ of random response with upper specification limit $y_g := \{Y|g(X) = 0\}$.

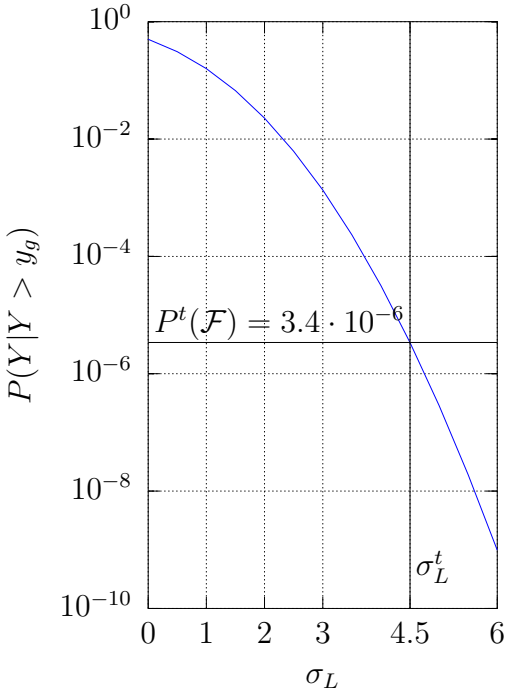

Figure 7: Sigma level variation and associated probability of failure (assumption: normal distribution for all important random responses).

maximum entropy method or saddlepoint expansion, as reviewed in Hurtado (2008), are frequently used within the reliability-based structural optimization replacing the expensive reliability analysis.

A more simple, non-intrusive approach for a rough estimation of the failure probability is the calculation of the minimal sigma level σ_L for a performance-relevant random response parameter Y defined by an upper and lower limitstate value $y_g^{u,l} := \{Y|g(X) = 0\}$ as follows

$$E[Y] \pm \sigma_L \cdot \sigma_Y \overset{!}{\leqq} y_g^{u,l}$$

The sigma level can be used in conjunction with standard deviation to measure the deviation of response values Y from the mean $E[Y]$. For example, for a pair of quantiles (symmetrical case) and the mean value we obtain the assigned sigma level

$$\sigma_L = \frac{y_g - E[Y]}{\sigma_Y} \tag{10}$$

of the limit state violation, as explained in Fig. 4. Therewith, the non-exceedance

probability results in

$$P(\mathcal{E}) = P(\{Y|Y \lesseqgtr y_g^{u,l}\}) = f(\sigma_L)$$

as a function of the sigma level, depending on the current distribution type of Y. In the same manner failure probability

$$P(\mathcal{F}) = P(\{Y|Y > y_g\}) = f(\sigma_L) \tag{11}$$

is given as a function of the sigma level. For example, assuming a normal distribution of the random response Y with $\mu_Y = 0$ and $\sigma_Y = 1$, as shown in Fig. 6, the failure probability is given as a nonlinear function

$$P(\mathcal{F}) = \Phi(-\sigma_L) = \Phi(-y_g)$$

of the sigma level, as illustrated in Fig. 7. Therewith, a probability of $P^t(\mathcal{F}) = 3.4 \cdot 10^{-6}$ is achieved when the performance target σ_L^t is 4.5 σ away from the mean value.

Other values of acceptable annual probabilities of failure $P^t(\mathcal{F})$ depending on the consequence of failure, significance warning or without warning before occurrence of failure and (non-)redundant structures can be found in engineering standards, e.g. in DNV (1992).

2.6 Methods solving stochastic optimization problems

In general, problem (1) to (6) is solved as a combination of a deterministic optimization in the n_d-dimensional design space and a stochastic analysis in the n_r-dimensional random space. Derivative-free global optimization methods are typically recommended to solve the sequential deterministic optimization problem, according to Eq. (1) for highly nonlinear numerical models, especially fluid-structure interaction models with probability-based constraints, whose objective and constraint function value may be computed with some noise or are non-computable in any design points.

Evolutionary computation, as a special class of global optimization strategies, imitates the natural processes like biological evolution or swarm intelligence. Based on the principle "survival of the fittest" a population of artificial individuals searches the design space of possible solutions in order to find a better solution for the optimization problem. In this paper an evolution strategy using a class of evolutionary algorithms is used. This strategy uses normally distributed mutations, recombination, selection of the best offspring individuals, and the principle of self-adaptation of strategy parameters, as described in Bäck (1995).

As an alternative derivative-free optimization method, especially useful for large real-life design optimization problems in which the objectives and constraints are

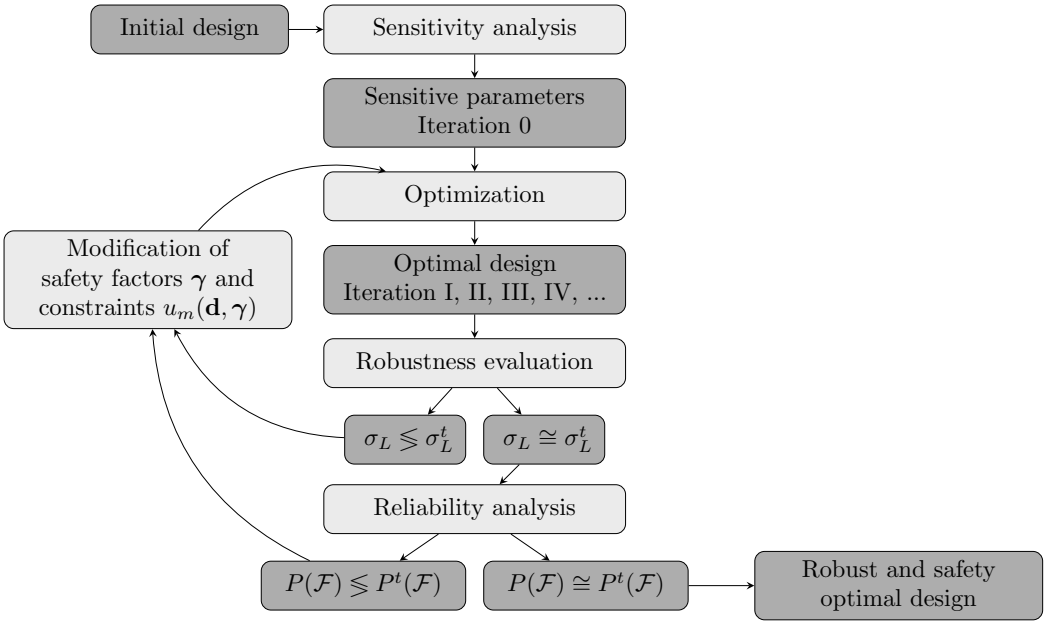

Figure 8: Basic concept of a decoupled loop of a reliability-based and variance-based stochastic design optimization using global variance-based sensitivity analysis and robustness evaluation to reduce the design parameter and random variable space.

determined as a result of very expensive numerical computations, we use the adaptive response surface methodology, as introduced in Etman et al. (1996), Toropov and Alvarez (1998), Abspoel et al. (1996), Stander and Craig (2002), Kurtaran et al. (2002).

Mainly, there are three methods for solving these kinds of coupled problems (1) to (6). The simplest and most direct solution method is a coupled approach in which a full reliability analysis is performed for every optimization function evaluation (see e.g. Choi et al., 2001). This involves a nesting of two distinct levels of optimization within each other, one at the design level and one at the reliability analysis level. However, despite progress in numerical methods to solve optimization problems and stochastic problems, this coupled procedure leads in general to an inefficient double loop with a large number of design evaluations. Alternatively, one way to overcoming this dilemma would be to use sensitivity analysis to analytically compute the design gradients.

The single-loop method (see e.g. Kharmanda et al., 2002) simultaneously minimizes the objective function and searches for the β-point, satisfying the probabilistic constraints only at the optimal solution, but needs a sensitivity analysis to analyti-

cally compute the design gradients of the probability constraint.

An alternative method, used in the following, is the sequential approach (see e.g. Chen et al., 2003). The general concept is to iterate between optimization and uncertainty quantification, updating the constraints based on the most recent probabilistic assessment results, using safety factors or other approximation methods. This effective iterative decoupled loop approach can be enhanced by updating the constraints during the internal optimization using sigma levels and statistical moments

$$\frac{\sigma_{L_k}}{\sigma_L^t} - 1 \geq 0;\ \sigma_{L_k} = \frac{y_{gk} - E[Y_k]}{\sigma_{Y_k}};\ k = 1, n_g$$

in place of the exceedance probability of the Eq. (3). Essentially, by means of transformation in Eq. (11) of the probability-based highly nonlinear and non-differentiable constraints to linear ones, these functions may be more well conditioned for the optimization approach and we can expect a better performance of the solution process. Of course, the transformation in Eq. (11) can only be used as a rough estimation of the safety level and we have to calculate the probabilities of failure using the reliability analysis, at least at the iteration end.

As shown in Fig. 8, in the initial iteration step a variance-based sensitive analysis identifies the most important multivariate dependencies and design parameters. After this, the deterministic optimization step results in an optimal solution for which the sigma level is calculated using a robustness evaluation, based on a latin hypercube sampling. The size of violation of the target sigma level is used to interpolate the constraints using modified safety factors. Whereby, as an important fact, the interpolation order increases continuously with each iteration step, so in practice three or four iteration steps may meet our optimization requirements in terms of robustness and safety. Fig. 5 shows a typical convergence of a sequential stochastic chance-constrained optimization.

Furthermore, the optimization steps and the final reliability analysis run mostly efficiently in the space of the current significant parameters. So every size of problem definition (number of design and random parameters) is solvable within all sigma levels.

The following numerical example with a very high degree of complexity is given to demonstrate the solving power of this sequential stochastic chance-constrained optimization by adapting the constraint $u_m(\mathbf{d}, \gamma)$ depending on interpolated nominal response values y_d.

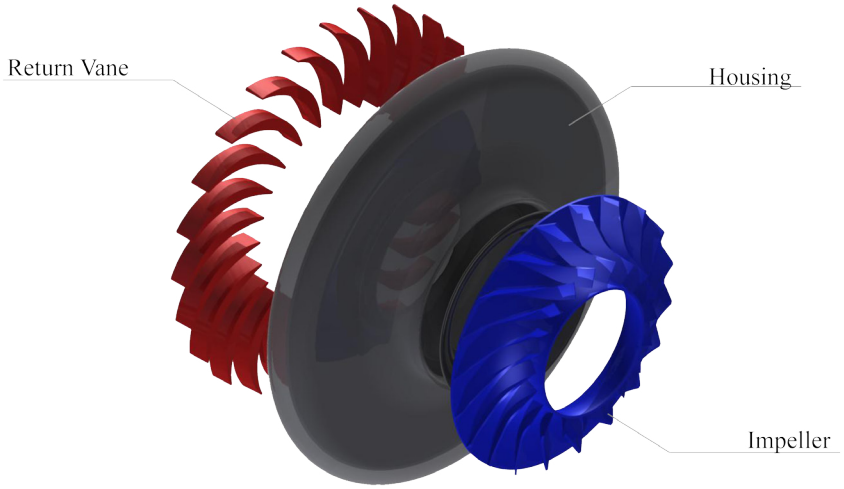

Figure 9: Parametric CAD model of a one stage radial compressor, consisting of a impeller and returnvane

3 NUMERICAL EXAMPLE

3.1 Computational fluid dynamics and process integration

Computational fluid dynamics (CFD) is an engineering method in which flow fields and other physics are calculated in detail for an application of interest. ANSYS, which is used for the following example, uses a multidisciplinary approach to simulation in which fluid flow models integrate seamlessly with other types of physics simulation technologies.

Whereas, the CAE integration was carried out with the ANSYS Workbench environment and optiPLug. The defined design and random parameters were modified with the software optiSLang for binary-based CAE process integration, distribution of the parallel Workbench processes and for optimization and stochastic analysis.

3.2 Fluid-structure interaction model

The stochastic optimization method presented here is applied to a CAD and CAE parameter-based design optimization of a radial compressor shown in Fig. 9, including material, process and geometry tolerances. In the example presented the target of the optimization process is to maximize the efficiency of the turbine engine with respect to a limitation of the maximal v. Mises stress. Additional constraints are defined by resonance of any eigen frequency with the rotational velocity of the rotor. In total

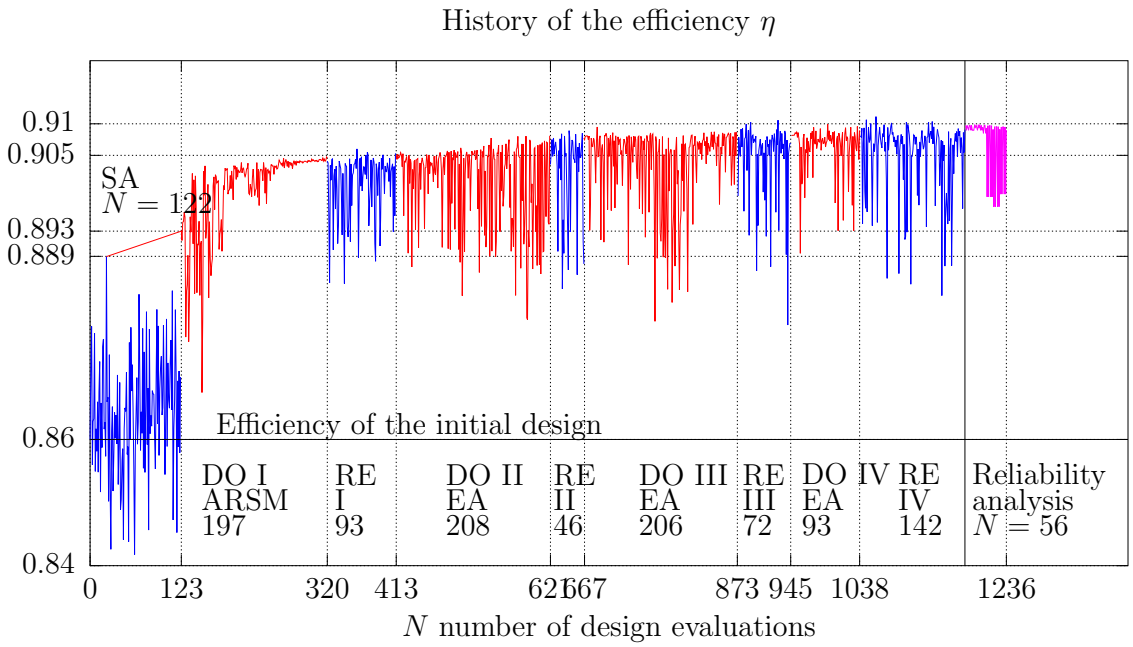

Figure 10: Overview for the history of the efficiency η of all iterations. DO=deterministic optimization, RE=Robustness evaluation, EA= Evolutionary algorithm, ARSM=Adaptive response surface method, SA=Sensitivity analysis

36 optimization parameters and 49 random influences are defined, as collected in Tab. 2.

3.3 Decoupled stochastic optimization loop

In the following the optimization loop presented in Fig. 8 will be shown. The initial step starts with the sensitivity analysis, based on the so called meta models of optimal prognosis. Therefore, the most important multivariate dependencies and design parameters can be identified (see Eq. (9)). With these parameters identified from the sensitivity analysis, the number of parameters related to the optimization problem can be reduced. In our case up to 10 design variables are left over with a relevant coefficient of optimal prognosis. Furthermore the meta models of optimal prognosis can be used as a surrogate model for a pre-optimization. The mean efficiency of the initial radial compressor was 86%. The best design of the latin hypercube sampling with an efficiency of 88.9% is used as start design of an evolutionary optimization based on the surrogate model and gives with one additional

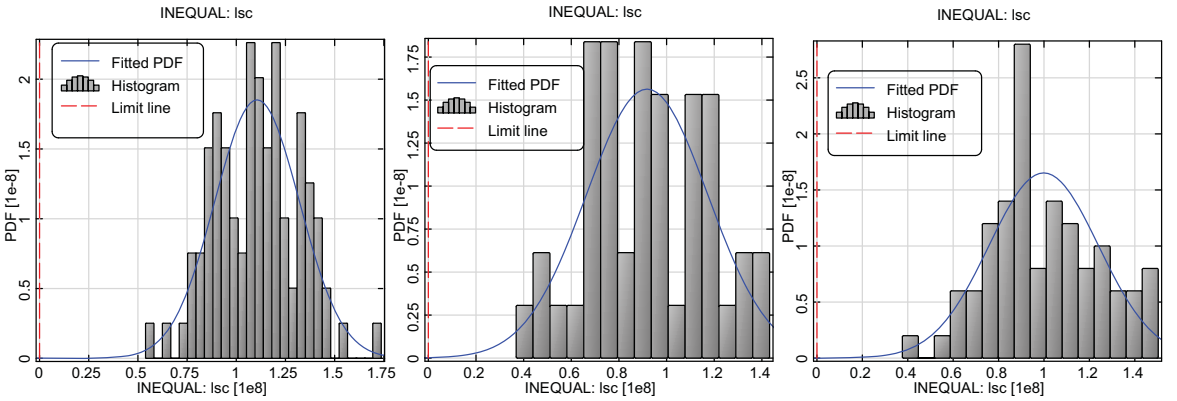

Statistic data			
Min:	5.388e+007	Max:	1.737e+008
Mean:	1.106e+008	Sigma:	2.154e+007
CV:	0.1948		
Skewness:	0.0605	Kurtosis:	2.924
Fitted PDF: Normal			
Mean:	1.106e+008	Sigma:	2.154e+007
Limit x = 0			
P_rel =	0	P_fit =	1.43132e-007
Probability P(X<x) = 0.95			
x_rel =	1.4365e+008	x_fit =	1.45998e+008

Figure 11: Iteration step I: Histogram of stress limit state $g^{\mathrm{I}} = \sigma_y^{\mathrm{I}} - \sigma_e^{\mathrm{I}}$.

Statistic data			
Min:	3.686e+007	Max:	1.432e+008
Mean:	9.182e+007	Sigma:	2.551e+007
CV:	0.2778		
Skewness:	0.007584	Kurtosis:	2.304
Fitted PDF: Normal			
Mean:	9.182e+007	Sigma:	2.551e+007
Limit x = 0			
P_rel =	0	P_fit =	0.000159682
Probability P(X<x) = 0.95			
x_rel =	1.32864e+008	x_fit =	1.33779e+008

Figure 12: Iteration step II: Histogram of stress limit state $g^{\mathrm{II}} = \sigma_y^{\mathrm{II}} - \sigma_e^{\mathrm{II}}$.

Statistic data			
Min:	3.762e+007	Max:	1.503e+008
Mean:	9.989e+007	Sigma:	2.415e+007
CV:	0.2418		
Skewness:	0.1299	Kurtosis:	2.601
Fitted PDF: Normal			
Mean:	9.989e+007	Sigma:	2.415e+007
Limit x = 0			
P_rel =	0	P_fit =	1.76654e-005
Probability P(X<x) = 0.95			
x_rel =	1.4367e+008	x_fit =	1.3961e+008

Figure 13: Iteration step III: Histogram of stress limit state $g^{\mathrm{III}} = \sigma_y^{\mathrm{III}} - \sigma_e^{\mathrm{III}}$.

design evaluation an efficiency of 89.3%. The first deterministic optimization in the sensitive design subspace results in the best deterministic design with an efficiency of 90.5%, as shown in Fig. 10.

After this, using a robustness evaluation, we can calculate the sigma level of the constraint violation with Eq. 10, for example regarding the stress. The distance of the design stress to the 5% quantile of the yield strength is a result of the first global safety factor of $\gamma^I = 1.5$ of the first iteration step. The target sigma level is $\sigma_L^t = 4.5$ to ensure a probability of failure $P(\mathcal{F}) = 3.14 \cdot 10^{-6}$. In our case after the first iteration, the sigma level is larger than the desired $\sigma_L^{\mathrm{I}} = 5.13 > 4.5$, therefore, a further iteration is necessary. In case of lack of prior knowledge, we use "rule of proportion" for the recalculation of the new safety factor (Fig. 14)

$$\gamma^{\mathrm{II}} = \gamma^{\mathrm{I}} \cdot \frac{\sigma_L^t}{\sigma_L^{\mathrm{I}}} = 1.32$$

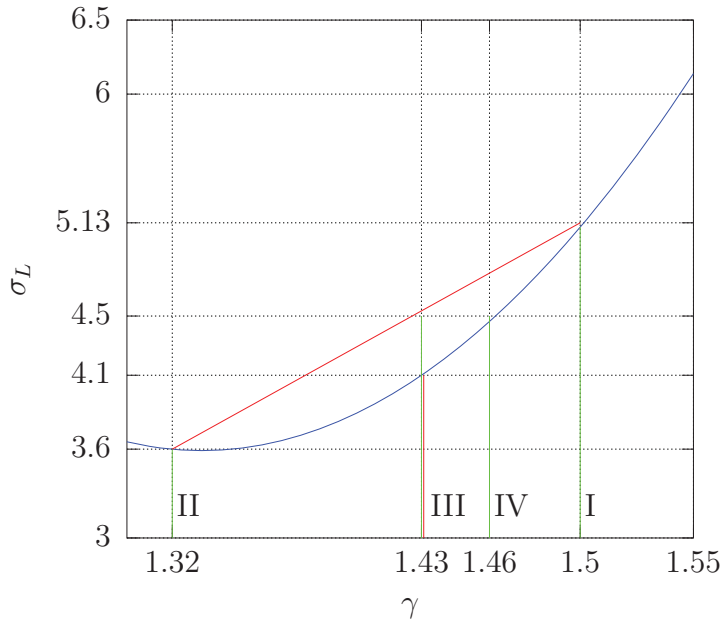

Figure 14: Interpolation of the global safety factor γ, depending on the estimated sigma level to modify the stress constraint, Eq. (2).

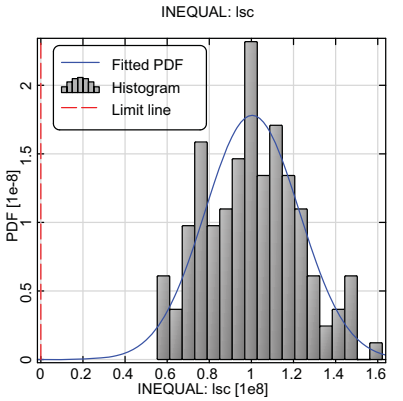

Statistic data			
Min:	5.527e+007	Max:	1.622e+008
Mean:	1.004e+008	Sigma:	2.24e+007
CV:	0.2231		
Skewness:	0.2139	Kurtosis:	2.7
Fitted PDF: Normal			
Mean:	1.004e+008	Sigma:	2.24e+007
Limit x = 0			
P_rel =	0	P_fit =	3.70381e-006
Probability P(X<x) = 0.95			
x_rel =	1.42685e+008	x_fit =	1.37226e+008

Figure 15: Iteration step IV: Histogram of stress limit state $g^{\mathrm{IV}} = \sigma_y^{\mathrm{IV}} - \sigma_e^{\mathrm{IV}}$.

The second deterministic optimization step increases the efficiency to 90.8% and the second robustness evaluation with a new nominal design stress results in a new mean and standard deviation of the violation of the stress limit state as shown in Fig. 12. But with these moments the new sigma level of $\sigma_L^{\mathrm{II}} = 3.6$ turns out to be less than the predicted sigma level. Now with the prior knowledge of the first iteration, we can interpolate the new global safety factor to $\gamma^{\mathrm{III}} = 1.426$ with a new nominal design stress $\sigma_d^{\mathrm{III}} = 1.75 \cdot 10^8$ for the third optimization.

After the third iteration, we obtain a new efficiency of 90.9% and the third robustness evaluation gives the following mean and standard deviation of the limit state violation shown in Fig. 13 with the new sigma level $\sigma_d^{\mathrm{III}} = 4.1 < 4.5$ near the target value. In the iteration step III now the interpolation order is a quadratic one and the new safety factor is $\gamma^{\mathrm{IV}} = 1.46$. With the resulting new nominal design stress $\sigma_d^{\mathrm{IV}} = 1.71 \cdot 10^8$

After the fourth iteration, we obtain the very best efficiency of 91%. In relation

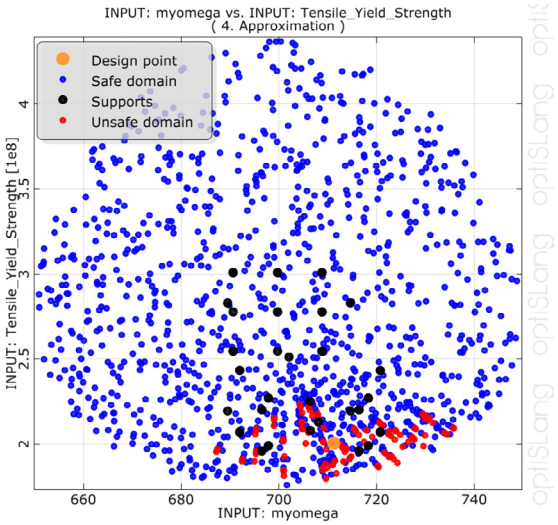

Figure 16: Anthill plot of the analyzed $N = 56$ design evaluations of the reliability analysis within iteration step IV between efficiency η and yield stress σ_y.

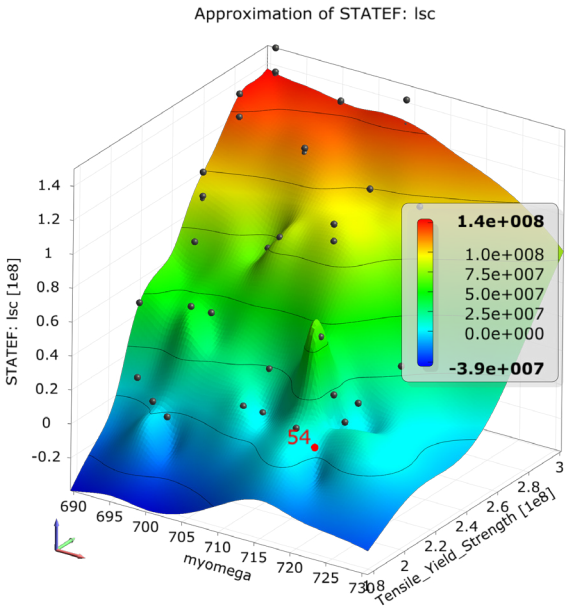

Figure 17: Response surface plot of the reliability analysis design IV.

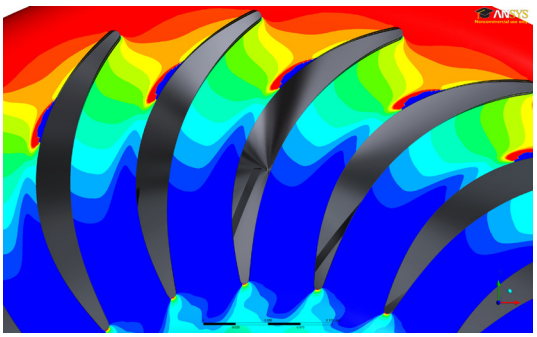

Figure 18: Flow angle of the initial design at the returnvane blades with separations along the blades

Figure 19: Flow angle of the optimized design at the returnvane blades with a much more uniform flow

to the initial design we have a better design performance of 5%. The final fourth robustness evaluation confirms the prediction of the sigma level $\sigma_L^{\mathrm{IV}} = 4.48 \approx 4.5$ and shows a small deviation of the efficiency as shown in Fig. 15.

Of course, the probability levels of violation of the limit state conditions or of the initial efficiency are only a rough estimation and at least a reliability analysis

of the final design is recommended, especially for small probability levels. With the identification of the random sub domain directional sampling on adaptive moving least square is used for reliability analysis (see Sec. 2.3). The moving least square approximation is based on $N = 56$ design evaluations of an adaptive D-optimal design of experiment, as shown in Figs. 16 and 17. A cluster analysis is used to detect only one failure domain with high failure probability. The directional sampling procedure on the surrogate model detects samples in the unsafe domain. The assigned failure probability $\bar{P}(\mathcal{F}) = 2.5 \cdot 10^{-6} \leq P^t(\mathcal{F}) = 3.4 \cdot 10^{-6}$ indicates an optimized six sigma design.

Finally, the Figs. 18 and 19 show the flow along the return vane blades. It is distinctly and visibly how the separations have been reduced in the optimized design and a more uniform flow is present.

4 CONCLUSIONS

Robust design optimization can provide multiple benefits. It permits the identification of those design parameters that are critical for the achievement of a certain performance characteristic. This can significantly reduce product costs. The effect of variations on the product behaviour and performance can be quantified. Moreover, robust design optimization can lead to a deeper understanding of the potential sources of variations. Consequently, more robust and affordable product designs can be achieved.

In this paper an efficient iterative decoupled loop approach is provided for reducing the necessary number of design evaluations. The applicability of this method for real case applications is demonstrated for a radial compressor. Using the approach presented, it is possible to improve the efficiency by about 5%. In addition we obtain an optimized design which is insensitive to uncertainties and considers the target failure probability.

5 ACKNOWLEDGEMENT

This project is kindly supported through the program “Internal Research Funding”, funded through the Niederrhein University of Applied Sciences. The authors would like to express their thanks to Johannes Einzinger of the ANSYS Germany GmbH for his assistance in formulating the FSI design problem and to Ulrike Adams and Daniela Ochsenfahrt of the DYNARDO GmbH for their support within the method implementation into the optiSLang software package and the collaborative work.

References

S.J. Abspoel, L.F.P. Etman, J. Vervoort, R.A. van Rooij, A.J.G Schoofs, and J.E. Rooda. Simulation based optimization of stochastic systems with integer design variables by sequential multipoint linear approximation. *Structural and Multidisciplinary Optimization*, 22:125–138, 1996.

T. Bäck. Evolution strategies: an alternative evolutionary algorithm. In *Artificial Evolution*, pages 3–20. Springer-Verlag, 1995.

A. Chateauneuf. *Advances in solution methods for reliability-based design optimization*, volume 1 of *Structures and Infrastructures: Structural Design Optimization Considering Uncertainties*, chapter 9, pages 217 – 246. Taylor & Francis, London, UK, 2008.

W. Chen, H. Liu, J. Sheng, and H. C. Gea. Application of the sequential optimization and reliabilty assessment method to structural design problems. In *Proceedings of DETC'03, ASME 2003 Design Engineering Technical Conferences and Computers and Information in Engineering Conference*, Chicao, Illinois USA, September 2 – 6 2003.

K. K. Choi, J. Tu, and Y. H. Park. Extensions of design potential concept for reliability-based design optimization to nonsmooth and extreme cases. *Structural and Multidisciplinary Optimization*, 22:335–350, 2001.

B. H. Dennis, G. S. Dulikravich, and Z.-X. Han. Constrined shape of optimization of airfoil cascades using a navier-stokes solver and a genetic/sqp algorithm. In *ASME 99-GT-441*, 1999.

O. Ditlevsen, R. E. Melchers, and H. Gluver. General multi-dimensional probability integration by directional simulation. *Computers & Structures*, 36:355–368, 1990.

DNV. Structural reliability analysis of marine structure. Technical Report Classification Notes, No. 30.6, Det Norske Veritas Classification AS, Computer Typesetting by Division Ship and Offshore, Norway, 1992.

L.F.P. Etman, J.M.T.A. Adriaens, M.T.P. van Slagmaat, and A.J.G. Schoofs. Crashworthiness design optimization using multipoint sequential linear programming. *Structural Optimization*, 12:222–228, 1996.

Victor E. Garzon. *Probabilistic Aerothermal Design of Compressor Airfoils*. PhD thesis, Massachusetts Institute of Technology, 2003.

Victor E. Garzon and David L. Darmofal. Impact of geometric variability on axial compressor performance. *Journal of Turbomachinery*, 125:692–703, 2003.

T. Homma and A. Saltelli. Importance measures in global sensitivity analysis of nonlinear models. *Reliability Engineering & System Safety*, 52(1):1 – 17, 1996.

D. E. Huntington and C. S. Lyrintzis. Improvements to and limitations of latin hypercube sampling. *Probabilistic Engineering Mechanics*, 13(4):245 – 253, 1998.

J. E. Hurtado. *Structural robustness and its relationship to reliability*, volume 1 of *Structures and Infrastructures: Structural Design Optimization Considering Uncertainties*, chapter 16, pages 435 – 470. Taylor & Francis, London, UK, 2008.

G. Kharmanda, A. Mohamed, and M. Lemaire. Efficient reliability-based design optimization using a hybrid space withapplication to finite element analysis. *Structural and Multidisciplinary Optimization*, 24:233 – 245, 2002.

H. Kurtaran, A. Eskandarian, D. Marzougui, and N.E. Bedewi. Crashworthiness design optimization using successive response surface approximations. *Computational Mechanics*, 29:409–421, 2002.

A. Lange, M. Voigt, K. Vogeler, H. Schrapp, E. Johann, and V. Gümmer. Probabilistic CFD simulation of a high-pressure compressor stage taking manufacturing variability into account. *ASME Conference Proceedings*, 2010(44014):617–628, 2010.

T. Most. Efficient sensitivity analysis of complex engineering problems. In M. H. Faber, J. Köhler, and K. Nishijima, editors, *11th International Conference on Applications of Statistics and Probability in Civil Engineering*, Zurich, 2011. Balkema.

T. Most and J. Will. Metamodel of optimal prognosis - an automatic approach for variable reduction and optimal metamodel selection. In *Proceedings of the 5th Weimar Optimization and Stochastic Days*, Weimar, Germany, November 20-21, 2008. DYNARDO GmbH.

J. Müller-Töws. *Aerodynamische Auslegung der Meridianströmung mehrstufiger Axialverdichter mit Hilfe von Optimierungsstrategien*. PhD thesis, Universität Kassel, 2000.

A. Oyama. Multidisciplinary optimization of transonic wing design based on evolutionary algorithms coupled with cfd solver. In *European Congress On Computational Methods In Applied Sciences And Engineering*, 2000.

R. Parchem and B. Meissner. Engine multidisciplinary optimization deployed on a two-stage turbine. In Ernst Kesseler, editor, *Advances in Collaborative Civil Aeronautical Multidisciplinary Design Optimization*, pages 289 – 331. AIAA, Amsterdam, The Netherlands, 2009.

S. Pierret and R. van den Braembussche. Turbomachinery blade design using a navier-stokes solver and artificial neural network. *Journal of Turbomachinery*, 121:326–332, 1999.

D. Roos. Multi-domain adaptive surrogate models for reliability analysis. In H. Budelmann, A. Holst, and D. Proske, editors, *Proceedings of the 9th International Probabilistic Workshop*, pages 191 – 207. Technical University Carolo-Wilhelmina zu Braunschweig, Braunschweig, Germany, November 17-18 2011.

A. Saltelli et al. *Global Sensitivity Analysis. The Primer*. John Wiley & Sons, Ltd, Chichester, England, 2008.

D. Sasaki, S. Obayashi, and H.-J. Kim. Evolutionary algorithm vs. adjoint method applied to sst shape optimization. In *The Annual Conference of CFD Society of Canada, Waterloo*, 2001.

S. Shahpar. A comparative study of optimisation methods for aerodynamic design of turbomachinery blades. In *Proceedings of ASME TURBOEXPO Nr. 2000-GT-523*, 2000.

Shyy, N. Wei, R. Papila, Vaidyanathan, and K. Tucker. Global design optimization for aerodynamics and rocket propulsion components. *Progress in Aerospace Sciences*, 71:59–118, 2001.

N. Stander and K.J. Craig. On the robustness of a simple domain reduction scheme for simulation-based optimization. *Eng. Comput.*, 19(4):431–50, 2002.

V. V. Toropov and L.F. Alvarez. Development of mars – multipoint approximation method based on the response surface fitting. Technical report, AIAA, 1998.

M. A. Trigg, G. R. Tubby, and A. G. Sheard. Automatic genetic optimization approach to 2d blade profile design for steam turbines. In *ASME 97-GT-392*, 1997.

Vaidyanathan, N. Rajkumar, W. Papila, K. Shyy, R. Tucker, L. Griffin, Haftka N., and Fitz-Coy. Neural network and response surface methodology for rocket engine component optimization. *AIAA*, pages 2000–4880, 2000.

A DESCRIPTION OF THE OPTIMIZATION PROBLEM

Response parameters of the initial and optimized Design					
o	**Description**	**Symbol**	Y_o^0	Y_o^{IV}	**Unit**
1	Total temperature ratio $\Theta_T = T_{\mathrm{t,inlet}}/T_{\mathrm{t,outlet}}$	Θ_{T}	1.1033	1.108	
2	Static entropy	S	0.013168	0.0088	
3	Air mass flow	$\dot{m}$	72.6	72.6	kg/s
4	Mechanical power	P	$-2.2664 \cdot 10^6$	$-2.3918 \cdot 10^6$	W
5	Resulting torque	τ	-3238.8	-3418.05	J
6	Flow angle inlet	$\alpha_{\mathrm{R_1}}$	2.2444	2.44	°
7	Flow angle between inlet and outlet	α_{RS}	62.562	67.63	°
8	Flow angle outlet	$\alpha_{\mathrm{S_1}}$	22.009	17.13	°
9	Isentropic efficiency	η	0.86	0.9094	
10	Pressure ratio $\Theta_P = P_{\mathrm{p,inlet}}/P_{\mathrm{p,outlet}}$	Θ_{P}	1.347	1.38	
11	Maximal displacement	$u_{\max}$	0.000111	0.000169	m
12	Von Mises stress	σ_{e}	$1.3107 \cdot 10^8$	$1.653 \cdot 10^8$	Pa
13	Eigenfrequencies $(o = 14, ..., 45)$	$\mathrm{f_i}$	1500-3200	1500-3200	Hz
46	Minimum safety factor	γ	2.4453	1.51	

Table 1: Table of all output parameters

Random variables X_j and **design variables** d_i of the initial and optimized Design; Φ =normal- Λ =log-normal distribution

j	i	**Description**	**Symbol**	$d_i^0 = E[X_j^0]$	$d_i^{IV} = E[X_j^{\mathrm{IV}}]$	$F_X(x)$	$\frac{\sigma_X}{E[X]}$	d_{l_i}	d_{u_i}	**Unit**
01	01	Inlet width	l_{in}	53	50.35	Φ	0.1	47.7	58.3	mm
02	02	Exit width	l_{ex}	26	26.27	Φ	0.1	23.4	28.6	mm
03	03	Radius of the impeller	r_{imp}	305	305.13	Φ	0.1	285	305	mm
04	-	Total temperature inlet	$T_{t,inlet}$	313	313	Φ	0.1	-	-	K
05	-	Specific heat capacity	C_p	1004.4	1004.4	Φ	0.1	-	-	J/kg/K
06	-	Specific gas constant	R	287.1	287.1	Φ	0.1	-	-	J/kg/K
07	-	Massflow of the air at the inlet	$\dot{m}$	72.6	72.6	Φ	0.1	-	-	kg/s
08	-	Rotation speed of the impeller	Ω	699.76	699.76	Φ	0.1	-	-	radian/s
09	-	Total pressure inlet	$P_{p,inlet}$	1724000	1724000	Φ	0.1	-	-	Pa
10	04	Angle variation along hub of the rotor	β_{RHB_1}	-48	-51.15	Φ	-0.1	-52.8	-43.2	°
11	05	Angle variation along hub of the rotor	β_{RHB_2}	-25	-23.23	Φ	-0.1	-27.5	-22.5	°
12	06	Angle variation along hub of the rotor	β_{RHB_3}	-25	-24.51	Φ	-0.1	-27.5	-22.5	°

continued on next page ...

Random variables X_j and **design variables** d_i of the initial and optimized Design; Φ =normal- Λ =log-normal distribution

j	i	**Description**	**Symbol**	$d_i^0 = E[X_j^0]$	$d_i^{IV} = E[X_j^{\mathrm{IV}}]$	$F_X(x)$	$\frac{\sigma_X}{E[X]}$	d_{l_i}	d_{u_i}	**Unit**
13	07	Angle variation along shroud of the rotor	$\beta_{\mathrm{RSB_1}}$	-55	-65.57	Φ	-0.1	-60.5	-49	°
14	08	Angle variation along shroud of the rotor	$\beta_{\mathrm{RSB_3}}$	-30	-28.02	Φ	-0.1	-33	-27	°
15	09	Angle variation along shroud of the rotor	$\beta_{\mathrm{RSB_3}}$	-45	-47.7	Φ	-0.1	-49.5	-40.5	°
16	10	Thickness of the rotor blades (shroud leading edge)	$t_{\mathrm{R_{SLE}}}$	1	0.9	Φ	0.1	0.8	1.2	mm
17	11	(shroud trailing edge)	$t_{\mathrm{R_{STE}}}$	6	5.95	Φ	0.1	5.0	7.0	mm
18	12	(hub trailing edge)	$t_{\mathrm{R_{HTE}}}$	6	5.96	Φ	0.1	5.0	7.0	mm
19	13	(hub leading edge)	$t_{\mathrm{R_{HLE}}}$	1	0.99	Φ	0.1	0.8	1.2	mm
20	14	Describes the curvature of the vanes (hub)	$\beta_{\mathrm{RVH_1}}$	60	71.54	Φ	0.1	54	66	°
21	15	Describes the curvature of the vanes (shroud)	$\beta_{\mathrm{RVS_1}}$	60	64.92	Φ	0.1	50	70	°
22	16	Relative thickness of the returnvane along the shroud	$\beta_{\mathrm{RVS_1}}$	45	41.88	Φ	0.1	35	55	mm

continued on next page ...

Random variables X_j and **design variables** d_i of the initial and optimized Design; Φ =normal- Λ =log-normal distribution

j	i	**Description**	**Symbol**	$d_i^0 = E[X_j^0]$	$d_i^{IV} = E[X_j^{\mathrm{IV}}]$	$F_X(x)$	$\frac{\sigma_X}{E[X]}$	d_{l_i}	d_{u_i}	**Unit**
23	17	Relative thickness of the returnvane along the hub	$\beta_{\mathrm{RVH_1}}$	45	43.42	Φ	0.1	45	66	mm
24	-	Density of the steel material	ρ	7850	7850	Φ	0.03	-	-	kg/m^3
25	-	Youngs modulus of steel	E	$2 \cdot 10^{11}$	$2 \cdot 10^{11}$	Λ	0.03	-	-	
26	-	Poissons ratio	ν	0.3	0.3	Λ	0.1	-	-	
27	-	Coefficient of thermal expansion	h_c	$1.2 \cdot 10^{-5}$	$1.2 \cdot 10^{-5}$	Φ	0.04	-	-	C$^-$1
28	-	Reference temperature	T_{Ref}	22	22	Φ	0.06	-	-	C
29	-	Tensile yield strength	σ_y	$2.5 \cdot 10^8$	$2.5 \cdot 10^8$	Λ	0.064	-	-	Pa
30	-	Compressive yield strength	σ_c	$2.5 \cdot 10^8$	$2.5 \cdot 10^8$	Λ	0.064	-	-	Pa
31	18	Describes the curvature of the vanes (shroud)	$\beta_{\mathrm{RVS_2}}$	0	-0.36	Φ	-0.1	-1	1	°
32	19	Describes the curvature of the vanes (shroud)	$\beta_{\mathrm{RVS_3}}$	0	-0.56	Φ	-0.1	-1	1	°
33	20	Relative thickness of the returnvane along the shroud	$t_{\mathrm{RVS_2}}$	10	10.88	Φ	0.1	8	12	mm

continued on next page ...

Random variables X_j and **design variables** d_i of the initial and optimized Design; Φ =normal- Λ =log-normal distribution

j	i	**Description**	**Symbol**	$d_i^0 = E[X_j^0]$	$d_i^{IV} = E[X_j^{\mathrm{IV}}]$	$F_X(x)$	$\frac{\sigma_X}{E[X]}$	d_{l_i}	d_{u_i}	**Unit**
34	21	Relative thickness of the returnvane along the shroud	t_{RVS_3}	6	6	Φ	0.1	4.8	4.8	mm
35	22	Describes the curvature of the vanes (hub)	β_{RVH_2}	0	-0.34	Φ	-0.1	-1	1	°
36	23	Describes the curvature of the vanes (hub)	β_{RVH_3}	0	-0.14	Φ	-0.1	-1	1	°
37	24	Relative thickness of the returnvane along the hub	t_{RVH_2}	6	6.17	Φ	0.1	4.8	7.2	mm
38	25	Relative thickness of the returnvane along the hub	t_{RVH_3}	10	12	Φ	0.1	8	12	mm
39	26	Axial ratio of the major axis to minor axis of the elliptical rounding of the inflow edge (hub)	r_{IEH}	3	3.12	Φ	0.1	2.4	3.6	

continued on next page ...

Random variables X_j and **design variables** d_i of the initial and optimized Design; Φ =normal- Λ =log-normal distribution

j	i	**Description**	**Symbol**	$d_i^0 = E[X_j^0]$	$d_i^{IV} = E[X_j^{\mathrm{IV}}]$	$F_X(x)$	$\frac{\sigma_X}{E[X]}$	d_{l_i}	d_{u_i}	**Unit**
40	27	Axial ratio of the major axis to minor axis of the elliptical rounding of the inflow edge (shroud)	$r_{\mathrm{I_{ES}}}$	3	3.14	Φ	0.1	2.4	3.6	
41	28	Edge of the vane at the leading edge along the hub contour	$r_{\mathrm{RV_{EHIn}}}$	1	0.99	Φ	0.1	0.8	1.2	
42	29	Edge of the vane at the leading edge along the shroud contour	$r_{\mathrm{RV_{ESIn}}}$	1	1	Φ	0.1	0.8	1.2	
43	30	Edge of the vane at the trailing edge along the hub contour	$r_{\mathrm{RV_{EHOut}}}$	1	1.03	Φ	0.1	0.8	1.2	
44	31	Edge of the vane at the trailing edge along the shroud contour	$r_{\mathrm{RV_{ESOut}}}$	1	1.18	Φ	0.1	0.8	1.2	
45	32	Hub to shroud offset impeller	$\xi_{\mathrm{I_{HTSO}}}$	0.5	0.53	Φ	0.1	0.4	0.6	%
46	33	Point tolerance impeller	$\xi_{\mathrm{I_{PT}}}$	0.1	0.08	Φ	0.1	0.08	0.12	%

continued on next page ...

Random variables X_j and **design variables** d_i of the initial and optimized Design; Φ =normal- Λ =log-normal distribution										
j	i	**Description**	**Symbol**	$d_i^0 = E[X_j^0]$	$d_i^{IV} = E[X_j^{\mathrm{IV}}]$	$F_X(x)$	$\frac{\sigma_X}{E[X]}$	d_{l_i}	d_{u_i}	**Unit**
47	34	Hub to shroud offset returnvanve	$\xi_{\mathrm{R_{HTSO}}}$	0.5	0.53	Φ	0.1	0.4	0.6	%
48	35	Point tolerance returnvane	$\xi_{\mathrm{R_{PT}}}$	0.1	0.08	Φ	0.1	0.08	0.12	%
49	36	Rounding of the trailing edge	r_{TE}	0.4	0.32	Φ	0.1	0.32	0.48	mm

Table 2: Table of all parameters

Constraints $u_m(\mathbf{d})$ **and objective** $f(\mathbf{d})$			
Type	**Description**	**Formula**	**Unit**
Constraint	$\gamma \geq 1.5$	$u_1(\mathbf{d}) = \gamma - 1.5$	
Constraint	Minimum of $\Theta_P \geq 1.34$	$u_2(\mathbf{d}) = \Theta_P - 1.34$	
Constraint	$\Omega/2\pi$ needs to be $\pm 10\%$ away of f_i	$u_3(\mathbf{d}) = \lvert(f_i - (\Omega/2\pi))/(\Omega/2\pi)\rvert - 0.1$	
Constraint	Ω/π needs to be $\pm 10\%$ away of f_i	$u_4(\mathbf{d}) = \lvert(f_i - (\Omega/\pi))/(\Omega/\pi)\rvert - 0.1$	
Limit state condition	Condition to calculate sigma level	$g_1(\mathbf{x}) = \sigma_y - \sigma_e$	Pa
Objective	Maximal efficiency (isentropic)	$f(\mathbf{d}) = \eta = \frac{\left(\frac{p_2}{p_1}\right)^{\frac{\kappa-1}{\kappa}} - 1}{\frac{T_2}{T_1} - 1}$	

Table 3: Table of all constraints and objectives